Article

Formation and Cleavage of Aromatic Disulfide Radical Anions

Sabrina Antonello, Kim Daasbjerg, Henrik Jensen, Ferdinando Taddei, and Flavio Maran

J. Am. Chem. Soc., **2003**, 125 (48), 14905-14916• DOI: 10.1021/ja036380g • Publication Date (Web): 04 November 2003

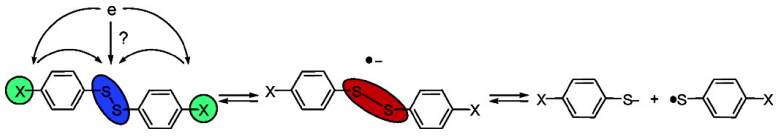

More About This Article

Additional resources and features associated with this article are available within the HTML version:

- Supporting Information
- Links to the 7 articles that cite this article, as of the time of this article download
- Access to high resolution figures
- Links to articles and content related to this article
- Copyright permission to reproduce figures and/or text from this article

View the Full Text HTML

J|A|C|S
ARTICLES
Published on Web 11/04/2003

Formation and Cleavage of Aromatic Disulfide Radical Anions

Sabrina Antonello,[†] Kim Daasbjerg,*[,‡] Henrik Jensen,[‡] Ferdinando Taddei,*[,§] and Flavio Maran*[,†]

Contribution from the Dipartimento di Chimica Fisica, Università di Padova, via Loredan 2, 35131 Padova, Italy, Department of Chemistry, University of Aarhus, DK-8000 Aarhus C, Denmark, and Dipartimento di Chimica, Università di Modena e Reggio Emilia, via Campi 183, 41100 Modena, Italy

Received May 28, 2003; E-mail: f.maran@chfi.unipd.it

Abstract: The electron transfer (ET) to a series of para-substituted diaryl disulfides, having the general formula $(X-C_6H_4S-)_2$, has been studied. The X groups were selected as to have a comprehensive variation of the substituent effect, being X = NH_2, MeO, H, F, Cl, CO_2Et, CN, and NO_2. The reduction was carried out experimentally, using *N,N*-dimethylformamide as the solvent, and by molecular orbital (MO) ab initio calculations. The ET was studied heterogeneously, by voltammetric reduction and convolution analysis, and homogeneously, by using electrogenerated radical anions as the solution electron donors. The reduction is dissociative, leading to the cleavage of the S−S bond in a stepwise manner. Both experimental approaches led us to estimate the E° and the intrinsic barrier values for the formation of the radical anions. Comparison of the independently obtained results allowed obtaining, for the first time, a quantitative description of the correlation between heterogeneous and homogeneous rate constants of ETs associated with significant inner reorganization energy. The experimental outcome was fully supported by the theoretical calculations, which provided information about the disulfide lowest unoccupied MOs (LUMOs) and singly occupied MO (SOMO), the bond dissociation energies, and the most significant structural modifications associated with radical anion formation. With disulfides bearing electron-donating or mildly electron-withdrawing groups, the inner reorganization is particularly large, which reflects the significant stretching of the S−S bond experienced by the molecule upon ET. The process entails formation of loose radical anion species in which the SOMO is heavily localized, as the LUMO, onto the frangible bond. As a consequence of the formation of these σ^*-radical anions, the S−S bond energy of the latter is rather small and the cleavage rate constant is very large. With electron-withdrawing groups, the extent of delocalization of the SOMO onto the aryl system increases, leading to a decrease of the reorganization energy for radical anion formation. Interestingly, while the LUMO now has π^* character, the actual reduction intermediate (and thus the SOMO) is still a σ^*-type radical anion. With the nitro-substituted disulfide, very limited inner reorganization is required and a π^*-radical anion initially forms. A nondissociative type intramolecular ET then ensues, leading to the formation of a new radical anion whose antibonding orbital has similar features as those of the SOMO of the other diaryl disulfides. Therefore, independently of the substituent, the actual S−S bond cleavage occurs in a quite similar way along the series investigated. The S−S bond cleavage rate, however, tends to decrease as the Hammett σ increases, which would be in keeping with an increase of both the electronic and solvent reorganization energies.

Introduction

Electron transfer (ET) processes are associated with structural and electronic changes of the species involved and with reorganization of the surrounding solvent molecules.[1,2] The sum of these contributions constitutes the intrinsic barrier ($\Delta G_0^{\ddagger}$), which is the free energy change necessary to bring the reactant system to the transition state for an ET reaction having zero driving force. For some molecular systems, electron uptake by an acceptor species (AB) causes the breaking of a σ bond to yield a radical ($A^\bullet$) and an anion (B^-).[3−5] Most often, the resulting dissociative ET mechanism is stepwise, and thus a radical anion ($AB^{\bullet-}$) is involved in the reaction sequence as a discrete intermediate (eqs 1 and 2). Sometimes, however, the energy of the reacting system is such that ET and bond cleavage can be even concerted (eq 3).

$$A-B + e \rightleftarrows A-B^{\bullet-} \quad (1)$$

$$A-B^{\bullet-} \rightarrow A^\bullet + B^- \quad (2)$$

$$A-B + e \rightarrow A^\bullet + B^- \quad (3)$$

To distinguish between the two mechanisms, the extent of the reorganization energy involved is, as a rule, the most important parameter. Simple outersphere ET reactions can be described

[†] Università di Padova.
[‡] University of Aarhus.
[§] Università di Modena e Reggio Emilia.

(1) Marcus, R. A.; Sutin, N. *Biochim. Biophys. Acta* **1985**, *811*, 265.
(2) *Electron Transfer: From Isolated Molecules to Biomolecules*; Jortner, J., Bixon, M., Eds.; Wiley: New York, 1999; Part 1.

10.1021/ja036380g CCC: $25.00

Scheme 1

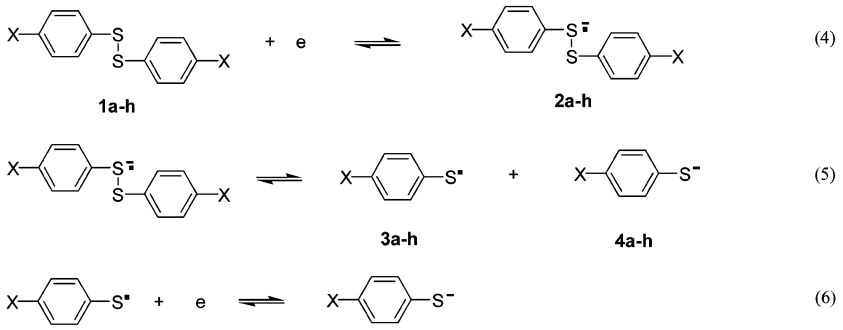

X = NH_2 (**1a**), MeO (**1b**), H (**1c**), F (**1d**), Cl (**1e**), CO_2Et (**1f**), CN (**1g**) and NO_2 (**1h**)

according to the Marcus model, in which the overall reorganization energy and thus intrinsic barrier are partitioned into solvent ($\Delta G^{\ddagger}_{0,s}$) and inner ($\Delta G^{\ddagger}_{0,i}$) components.[1] If the ET product is a delocalized aromatic radical anion, little molecular deformation occurs and thus $\Delta G^{\ddagger}_{0,i}$ is small. In this case, $\Delta G^{\ddagger}_{0,s}$ is the most important contribution to the intrinsic barrier.[6] $\Delta G^{\ddagger}_{0,i}$, however, is expected to increase when the ET causes bond fragmentation. This is particularly true for the concerted process (eq 3) in which $\Delta G^{\ddagger}_{0,i}$ becomes as large as one-fourth of the bond dissociation energy (BDE) of the breaking bond.[7] In fact, for this type of mechanism, $\Delta G^{\ddagger}_{0,i}$ is responsible for 70−80% of the overall barrier. In general, if we consider a dissociative ET involving the transient formation of a radical anion, it is reasonable to expect that the breaking bond will weaken and stretch to some extent because of the antibonding nature of the singly occupied molecular orbital (SOMO).

Very recently, we showed that the reduction of disulfides[8−10] provides striking examples of stepwise dissociative ETs endowed by a significant inner reorganization.[11] MO ab initio calculations, carried out for a variety of symmetrical and unsymmetrical disulfides,[10] showed that the large $\Delta G^{\ddagger}_{0,i}$ values observed are due to the significant elongation (0.8 Å) undergone by the S−S bond upon formation of the radical anion. The peculiarity of this type of reduction mechanism, which we define as the loose radical-ion dissociative ET mechanism, is that the electron uptake has an intrinsic barrier that is closer to that of a concerted dissociative ET than to that of the ET step of common stepwise processes. Our calculations could also show that the large reorganization energy observed is a consequence of the formation of σ^*-radical anions. This is in agreement with previous information on these anionic disulfide species[12] and with the result of similar calculations.[13] On the other hand, for the most common case of stepwise dissociative ETs, in which the unpaired electron is initially located into a π^* orbital, $\Delta G^{\ddagger}_{0,i}$ can be indeed negligible compared to $\Delta G^{\ddagger}_{0,s}$.[5] Even though our present state of knowledge is rather satisfactory, additional information is still required to better define both the loose radical-ion dissociative ET mechanism and the "gray" situations connecting it to the "normal" stepwise behavior. Understanding these features will ultimately improve our capability of predicting the dissociative ET rate for a much wider range of specific molecular systems.

In this paper, we describe experimental results and theoretical calculations on the reduction of an extended series of *para*-substituted diaryl disulfides **1** that provide important insights into the dynamics of borderline stepwise dissociative ETs. Compounds **1** undergo the stepwise reduction mechanism illustrated in Scheme 1.[9] Along with the reduction (eq 4) and radical-anion cleavage (eq 5) steps, Scheme 1 includes also the reduction of the thiyl radicals **3** to the thiolate anions **4**. In fact, at the rather negative reduction potentials of compounds **1**, reaction 6 is generally favored by at least 1 V.

The reduction was studied by electrochemistry and MO ab initio calculations. The kinetic experiments were carried out in *N*,*N*-dimethylformamide (DMF). The ET was studied heterogeneously, by voltammetric reduction and convolution analysis, and homogeneously, by using electrogenerated radical anions as the electron donors. Both methods allowed us to estimate the intrinsic barriers for the formation of the radical anions **2**. The heterogeneous and homogeneous ET results indicated that the intrinsic barrier is provided mostly by the inner component, unless good electron-withdrawing substituents are present in the molecule. The results were fully supported by the ab initio calculations that we carried out on a representative group of disulfides (**1a**, **1c**, **1d**, **1g**, and **1h**) and corresponding radical anions **2**, radicals **3**, and anions **4**. The data suggested that for the majority of the compounds investigated a simple representation in terms of reactant and product Morse curves would give only a rough molecular description of how ET and S−S bond cleavage take place. Most important, the theoretical results provided a detailed description of the substituent effect on the

(3) Savéant, J.-M. In *Advances in Electron-Transfer Chemistry*; Mariano, P. S., Ed.; JAI Press: Greenwich, CT, 1994; Vol. 4, p 53.
(4) Eberson, L. *Acta Chem. Scand.* **1999**, *53*, 751.
(5) Maran, F.; Wayner, D. D. M.; Workentin, M. S. *Adv. Phys. Org. Chem.* **2001**, *36*, 85.
(6) Typical values of $\Delta G^{\ddagger}_{0,s}$ and $\Delta G^{\ddagger}_{0,i}$ are of the order of 3−5 and 1 kcal mol^{-1}, respectively. For example, see: (a) Eberson, L. *Electron-Transfer Reactions in Organic Chemistry*; Springer-Verlag: Heidelberg, 1987. (b) Larsen, H.; Pedersen, S. U.; Pedersen, J. A.; Lund, H. *J. Electroanal. Chem.* **1992**, *331*, 971. (c) Jürgen, D.; Pedersen, S. U.; Pedersen, J. A.; Lund, H. *Acta Chem. Scand.* **1997**, *51*, 767.
(7) Savéant, J.-M. *J. Am. Chem. Soc.* **1987**, *109*, 6788.
(8) Christensen, T. B.; Daasbjerg, K. *Acta Chem. Scand.* **1997**, *51*, 307.
(9) Daasbjerg, K.; Jensen, H.; Benassi, R.; Taddei, F.; Antonello, S.; Gennaro, A.; Maran, F. *J. Am. Chem. Soc.* **1999**, *121*, 1750.
(10) Antonello, S.; Benassi, R.; Gavioli, G.; Taddei, F.; Maran, F. *J. Am. Chem. Soc.* **2002**, *124*, 7529.
(11) The observation of rather large $\Delta G^{\ddagger}_{0,i}$ values is not a specific property of the reduction of disulfides but has been observed also with some sulfides (Severin, M. G.; Arévalo, M. C.; Maran, F.; Vianello, E. *J. Phys. Chem.* **1993**, *97*, 150. Jakobsen, S.; Jensen, H.; Pedersen, S. U.; Daasbjerg, K. *J. Phys. Chem. A* **1999**, *103*, 4141) and for the dissociative oxidation of oxalate (Isse, A. A.; Gennaro, A.; Maran, F. *Acta Chem. Scand.* **1999**, *53*, 1013).
(12) Armstrong, D. A.; Chipman, D. M. In *S-centered Radicals*; Alfassi, Z. B., Ed.; Wiley: Chichester, U.K., 1999; pp 1−26.
(13) Carles, S.; Lecomte, F.; Schermann, J. P.; Desfrançois, C.; Xu, S.; Nilles, J. M.; Bowen, K. H.; Bergès, J.; Houée-Levin, C. *J. Phys. Chem. A* **2001**, *105*, 5622. See also: Braïda, B.; Thogersen, L.; Wu, W.; Hiberty, P. C. *J. Am. Chem. Soc.* **2002**, *119*, 11781.

reaction mechanism. We found that the energies and character of the lowest unoccupied molecular orbitals (LUMOs) and of the SOMOs change significantly along the series. Electron-donating and mildly electron-withdrawing substituents make both the LUMO and the SOMO display a pronounced σ^* character. On the other hand, with more powerful electron-withdrawing substituents, while the LUMO is a π^* orbital, it becomes a σ^*-type SOMO because of the large S−S bond elongation. Eventually, with the nitro substituent, the energy of the π^* LUMO is such that the SOMO also is a π^* orbital. Nevertheless, upon S−S bond elongation, a new SOMO, displaying the same features observed with the other substituents, was characterized. Therefore, independently of the disulfide, the actual S−S bond fragmentation involves a σ^*-type radical anion and occurs through a thermally activated endergonic reaction.

Experimental Section

Chemicals. *N*,*N*-Dimethylformamide (Acros Organics, 99%) was treated for some days with anhydrous Na_2CO_3, under stirring, and then distilled at reduced pressure (17 mmHg) under a nitrogen atmosphere. Tetrabutylammonium perchlorate (Fluka, 99%) was recrystallized from a 2:1 ethanol−water solution. Tetrabutylammonium tetrafluoroborate was prepared by reacting sodium tetrafluoroborate with tetrabutylammonium hydrogensulfate in water. It was recrystallized from dichloromethane. The syntheses of the disulfides were carried out according to the procedure outlined in ref 14. The purity was confirmed by means of ^{1}H NMR and GC−MS. The mediators were commercially available or prepared as described elsewhere.[15]

Electrochemical Apparatus. The electrochemical measurements were conducted in all glass cells. For direct electrochemistry (cyclic voltammetry and convolution analysis), an EG&G-PARC 173/179 potentiostat-digital coulometer, an EG&G-PARC 175 universal programmer, and a Nicolet 3091 12-bit resolution digital oscilloscope were used. To minimize the electrical noise, the experiments were carried out inside a double-wall copper Faraday cage, using the various precautions described in detail previously.[16] For the redox catalysis measurements, the experimental setup and procedures were as previously described.[17] For both types of experiment, the feedback correction was applied to minimize the ohmic drop between the working and the reference electrodes.

The electrochemical experiments were carried out in DMF containing 0.1 M Bu_4NClO_4 (TBAP), direct reduction, or 0.1 M Bu_4NBF_4 (TBAT), mediated reduction, using a glassy-carbon working electrode and a platinum plate as the counter electrode. A platinum electrode was employed for the oxidation studies. The reference electrode (either Ag/AgCl or Ag/AgI) was calibrated after each experiment against the ferrocenium/ferrocene couple. All potentials were then converted to the KCl saturated calomel electrode (SCE). The reference and the counter electrodes were separated from the catholyte by glass frits and Tylose-TBAP-saturated bridges.

Electrochemical Procedures. For the determination of the heterogeneous parameters, the digitalized, background-subtracted curves were analyzed by using a homemade voltammetry-convolution software and compared with the corresponding digital simulations. The DigiSim 3.03 package was used for the simulations, using a step size of 1 mV and an exponential expansion factor of 0.5. The standard potentials of the substituted phenylthiyl radicals **3** (eq 6) were determined by digital simulation of the experimental cyclic voltammetric curves for oxidation of the corresponding thiophenoxide ions **4**. The anions were generated by electroreduction of the parent disulfide and also chemically, by reaction of the pertinent thiophenol with tetrabutylammonium hydroxide. The results obtained by the two methods agreed with each other.

The rate constants for the homogeneous reaction between series of aromatic radical anion donors and **1a−d,f−h** were measured by different electrochemical techniques. Whereas cyclic voltammetry (CV) and linear scan voltammetry (LSV) were the electrochemical techniques of choice for the reactions having rate constants (k_{hom}) larger than 1 M^{-1} s^{-1}, we employed a potentiostatic technique for the study of the reactions having $k_{hom} = 10^{-3}-10$ M^{-1} s^{-1}.[17] To attain the situation in which the reaction kinetics was controlled solely by the forward ET from the radical anion to the disulfide (eq 4, in which "e" symbolizes the reductant), the experiments were usually carried out at low mediator concentrations (1−2 mM). For the radical anion of **1h**, however, the cleavage in eq 5 was so slow that mediator concentrations as low as 0.2−0.5 mM had to be employed, leading to a higher uncertainty in the determination of k_{hom}. Moreover, when the potentiostatic method was used in the study of the slow reactions, methyl *p*-toluenesulfonate was added to the solution in order to trap in a fast S_N2 reaction the thiophenoxides formed in steps 5 and 6. Thereby, any influence on the reaction kinetics from the reverse reaction of eq 5 and accordingly from the fast and usually diffusion-controlled backward ET involving **2** and the mediator could be neglected. In this respect, the rate measurements carried out by the CV and LSV techniques are less influenced because the reaction between **2** and the mediator is less exergonic and thus generally slower.

Computational Details. The calculations were performed at the MO ab initio level with the Gaussian 98 series of programs[18] run on a Silicon Graphics 4CPU MIPS R10000, SGI-ORIGIN 2000/16, and CRAY T3D MCA 128-8 supercomputer. The molecules **1** and anions **4** were studied at the HF/6-311G*//HF/6-311G* level, while the corresponding unrestricted UHF scheme was employed for the open-shell species **2** and **3**. Stationary points were located through full geometry relaxation. The single-point frozen core (f.c.) MP2 energies also were obtained. For the open-shell systems, the spin projection operator[19] was applied to remove contamination from higher spin states. For several of the radicals examined, however, the value of $\langle s^2 \rangle$ was greater than 0.75. The solvent effect (having $\epsilon = 37$) on the total molecular energy was estimated by using the Self-Consistent Reaction Field (SCRF) facility employing the polarized continuum model (PCM) performed with the Onsager reaction field theory and implemented in the Gaussian 98 package. The energy profiles were constructed as Morse-like potential energy functions of the S−S bond distance by employing the second derivative of the molecular energy corresponding to the relaxed molecular structure, with respect to the S−S bond length coordinate, following a procedure reported previously.[20] While the energy profiles were obtained by employing the energy of the critical points at the MP2/6-311G*//HF/6-311G* level, the exponential β factors were calculated at the HF/6-311G*//HF/6-311G* level (the unrestricted UHF scheme was used for the radical anions).

(14) (a) Bogert, M. T.; Stull, A. *Organic Synthesis*; New York, 1932; Vol. I. (b) Gundermann, K.-D.; Hümke, K. *Houben-Weyl*; Klamann, D., Ed.; Georg Thieme Verlag: Stuttgart, 1985; p 129.
(15) Occhialini, D.; Kristensen, J. S.; Daasbjerg, K.; Lund, H. *Acta Chem. Scand.* **1991**, *46*, 474.
(16) Antonello, S.; Musumeci, M.; Wayner, D. D. M.; Maran, F. *J. Am. Chem. Soc.* **1997**, *119*, 9541.
(17) Daasbjerg, K.; Pedersen, S. U.; Lund, H. *Acta Chem. Scand.* **1991**, *45*, 424.
(18) Frisch, M. J.; Trucks, G. W.; Schlegel, H. B.; Scuseria, G. E.; Robb, M. A.; Cheeseman, J. R.; Zakrzewski, V. G.; Montgomery, J. A., Jr.; Stratmann, R. E.; Burant, J. C.; Dapprich, S.; Millam, J. M.; Daniels, A. D.; Kudin, K. N.; Strain, M.; Farkas, C. O.; Tomasi, J.; Barone, V.; Cossi, M.; Cammi, R.; Mennucci, B.; Pomelli, C.; Adamo, C.; Clifford, S.; Ochterski, J.; Petersson, G. A.; Ayala, P.; Cui, Y. Q.; Morokuma, K. D.; Malick, K.; Rabuck, A. D.; Raghavachari, K.; Foresman, J. B.; Cioslowski, J.; Ortiz, J. V.; Baboul, A. G.; Stefanov, B. B.; Liu, G.; Liashenko, A.; Piskorz, P.; Komaromi, I.; Gomperts, R.; Martin, L. R.; Fox, D. J.; Keith, T.; Al-Laham, M. A.; Peng, C. Y.; Nanayakkara, A.; Gonzalez, C.; Challacombe, M.; Gill, P. M. W.; Johnson, B.; Chen, W.; Wong, M. W.; Andres, J. L.; Gonzalez, C.; Head-Gordon, M.; Replogle, E. S.; Pople, J. A. *Gaussian 98*, revision A.7; Gaussian, Inc.: Pittsburgh, PA, 1998.
(19) (a) Schlegel, H. B. *J. Chem. Phys.* **1986**, *84*, 4530. (b) Schlegel, H. B. *J. Phys. Chem.* **1988**, *92*, 3075. (c) Sosa, C.; Schlegel, H. B. *Int. J. Quantum Chem.* **1986**, *30*, 55.
(20) Benassi, R.; Taddei, F. *J. Phys. Chem. A* **1998**, *102*, 6173.

Table 1. Electrochemical and Kinetic Parameters for the Direct Reduction of Disulfides **1** and Oxidation of Anions **4** in DMF/0.1M TBAP at 25 °C

disulfide or thiophenoxide	$E_{p,1}$[a] (V)	α[b]	α[c]	α[d]	E_1°[e–g] (V)	log k_{het}°[e–g] (cm s^{-1})	$\Delta G^{\ddagger}_{0,het}$[h] (kcal mol^{-1})	$\Delta G^{\ddagger}_{0,i,het}$[i] (kcal mol^{-1})	r_1 (Å)	$E_{p,4}$[a] (V)	E_3°[j] (V)	ΔBDFE (kcal mol^{-1})
a	−1.86	0.336	0.422	0.410	−1.60	−3.95	10.3	6.6	3.8	−0.41	−0.37	28.4
b	−1.71	0.305	0.404	0.388	−1.38	−4.36	10.8	7.2	3.9	−0.14	−0.07	30.2
c	−1.65	0.325	0.434	0.414	−1.37	−4.22	10.7	6.8	3.6	−0.02	0.07	33.2
d	−1.55	0.336	0.404	0.408	−1.27	−3.84	10.1	6.3	3.7	0.03	0.12	32.1
e	−1.43	0.368	0.367	0.410	−1.18	−3.73	10.0	6.3	3.8	0.12	0.21	32.1
f	−1.23	0.364	0.508	0.482	−1.15	−2.69	8.5	5.2	4.2	0.28	0.37	35.1
g	−1.15	0.358	0.438	0.471	−1.06	−2.60	8.4	4.7	3.8	0.37	0.47	35.3
h	−0.79	0.610	0.734	0.726	−0.90	−0.80	5.9	2.3	3.9	0.42	0.53	33.0

[a] $\upsilon = 0.2$ V s^{-1}. [b] Calculated from $|\partial E_p/\partial \log \upsilon| = 1.15\ RT/F\alpha$. [c] Calculated from $\Delta E_{p/2} = 1.857 RT/F\alpha$. [d] Calculated from the convolution data for the midpoint potential of the peak width range, $E_p - 0.5\Delta E_{p/2}$, where $E_p = E_p$ (0.2 V s^{-1}). [e] From the convolution data. [f] From ref 9 (except for **1e**). [g] The experimental uncertainty associated with the parameters obtained for $\alpha = 0.5$ is 20−40 mV (E°) and 0.2−0.3 log units (log k_{het}°). [h] From $k_{het}^{\circ} = Z_{het} \exp(-\Delta G^{\ddagger}_{0,het}/RT)$. [i] Calculated by taking into account the solvent reorganization energy, obtained from the empirical equation $\Delta G^{\ddagger}_{0,s,het} = 13.9/r_1$ (Å). The error associated with these free energy estimates is of the order of 1 kcal mol^{-1}. [j] From simulation of the oxidation peak of **4**, the experimental uncertainty being ∼20 mV.

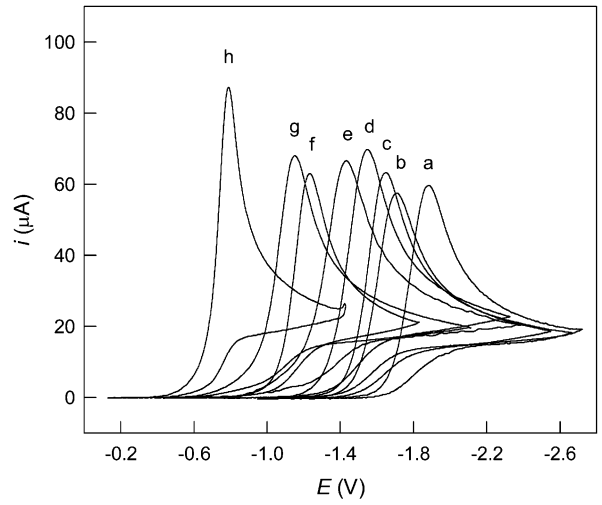

Figure 1. Reduction of disulfides **1a**−**h** (2 mM) in DMF/0.1 M TBAP at the glassy carbon electrode. Scan rate = 0.2 V s^{-1}; T = 25 °C.

Results

Electroreduction of Disulfides 1. The CV of the investigated disulfides is characterized by a reduction peak that is irreversible in the scan rate (υ) range employed, 0.1−200 V s^{-1}. The peak potential (E_p) strongly depends on the ring substituents, spanning a range of more than 1 V; this dependence is illustrated in Figure 1 and reported in Table 1. According to the mechanism described in Scheme 1, the reductive process is a two-electron process. For **1a**−**e**, the peak width (which is indicated as $\Delta E_{p/2}$ and is the difference between the potential measured at half-peak height and E_p) is in the range 110−130 mV at 0.2 V s^{-1}. The $\Delta E_{p/2}$ is related through the relationship $\Delta E_{p/2} = 1.857\ RT/F\alpha$[21] to the transfer coefficient α, which measures the sensitivity of the ET rate on ΔG° (i.e., $\alpha = \partial \Delta G^{\ddagger}/\partial \Delta G^{\circ}$). From the above $\Delta E_{p/2}$ values, we calculate α values in the range 0.367−0.434. For the disulfides with more powerful electron-withdrawing ring substituents, the irreversible peaks are sharper. For example, the $\Delta E_{p/2}$ values of **1f** and **1h** are 94 and 65 mV, respectively, which leads to calculated α values of 0.508 and 0.734. The same trend was verified by analyzing the scan rate dependence of the E_p value. For example, whereas for **1a**−**d** $\partial E_p/\partial \log \upsilon$ is between 88 and 97 mV/decade, corresponding to α values in the range 0.305−0.336 ($\partial E_p/\partial \log \upsilon = 1.15\ RT/F\alpha$),[21] the shift observed with **1h** is only 48 mV/decade and thus α increases to 0.610. The various α values are compared in Table 1. The α values obtained from $\Delta E_{p/2}$ are scan-rate dependent and so is the normalized peak current, $i_p/\upsilon^{1/2}$. Both parameters decrease as υ increases, pointing to a nonlinear dependence of the heterogeneous ET kinetics on the applied electrode potential, E.

The kinetics of the heterogeneous ET reactions of **1a**−**d**,**f**−**h** has been previously studied and reported[9] and thus only a brief summary of the procedures that allowed us to estimate the relevant ET parameters will be given. The analysis of the reduction of **1e** was carried out along similar lines. The heterogeneous parameters were obtained by applying the convolution analysis approach[5,16] to low-noise background-subtracted voltammograms recorded in the range of scan rates 0.1−20 V s^{-1}. Thus, convolution of the experimental curves, followed by logarithmic analysis of the resulting $I-E$ curves,[22] allows one to calculate the heterogeneous rate constant, k_{het}, as a function of E. The plots obtained for compounds **1a**−**h** displayed a nonlinear behavior. The determination of the apparent value of the transfer coefficient α was carried out by derivatization of the ln $k_{het} - E$ plots, being $\Delta G^{\circ} = F(E - E_1^{\circ})$ and thus $\alpha = -(RT/F)\ \partial \ln k_{het}/\partial E$. An estimate of the standard potential of the disulfides, E_1°, was obtained as the E value at which $\alpha = 0.5$. As we shall discuss in the following, for the particular dissociative ET reduction undergone by the disulfides, this procedure is liable to provide only a rough estimate of E° and thus the results displayed in Table 1 should be taken with some precaution. On the other hand, the relative values obtained for the various disulfides **1** (enforced by the analogous comparison of the homogeneous results; see below) are believed to be much more precise. The apparent values of the standard rate constant, k_{het}° (Table 1), were obtained by parabolic fit to the ln $k_{het} - E$ plots for $E = E_1^{\circ}$. By using these E_1° and k_{het}° estimates, we could simulate the experimental curves quite nicely in a wide range of υ values. The k_{het}° values vary

(21) Bard, A. J.; Faulkner, L. R. *Electrochemical Methods, Fundamentals and Applications*, 2nd ed.; Wiley: New York, 2001.

(22) The convoluted current I is related to the actual current i through the convolution integral, $I = \pi^{-1/2} \int_0^t (i(u)/(t-u)^{1/2})\ du$ (Imbeaux, J. C.; Savéant, J.-M. *J. Electroanal. Chem.* **1973**, *44*, 169). The $I-E$ plot has a sigmoidal shape, the limiting value being $I_l = nFAD^{1/2}C^*$, where n is the overall electron consumption, A, the electrode area, D, the diffusion coefficient, and C^*, the substrate concentration. If the heterogeneous ET is intrinsically slow or becomes irreversible because of a fast follow-up reaction (e.g., bond cleavage), the potential-dependent heterogeneous rate constant $k_{het} = k_{het}(E)$ is obtained as a function of E through equation $\ln k_{het}(E) = \ln D^{1/2} - \ln[(I_l - I)/i]$.

considerably along the series of disulfides, log k°_{het} going from −0.80 for **1h** to −4.36 for **1b**. Some of them, those of **1a**−**e**, are unusually low for substrates undergoing a stepwise dissociative ET mechanism. By using the Eyring equation and the pertinent nuclear frequency factor, Z_{het} ($Z_{het} = (RT/2\pi M)^{1/2}$, where M is the molar mass), we obtained the heterogeneous intrinsic barriers, $\Delta G^{\ddagger}_{0,het}$. Because of the large variation of k°_{het}, the $\Delta G^{\ddagger}_{0,het}$ also varies considerably. Table 1 shows both the $\Delta G^{\ddagger}_{0,het}$ values and the corresponding inner components, $\Delta G^{\ddagger}_{0,i,het}$. The latter was obtained from $\Delta G^{\ddagger}_{0,het}$ after correction for the solvent reorganization energy, $\Delta G^{\ddagger}_{0,s,het}$, which was obtained from the empirical equation that was derived[16] from an extensive set of experimental data,[23] that is, $\Delta G^{\ddagger}_{0,s,het} = 13.9/r_{\mathbf{1}}$ in which $r_{\mathbf{1}}$ (in angstroms) is the radius of the disulfide. The radii of **1a**−**h** were calculated by using as a reference value the radius of **1c**, 3.6 Å, which was obtained from the diffusion coefficient, 7.5×10^{-6} cm^2 s^{-1}, and the Stokes−Einstein equation. The radius of **1c** was in very good agreement (within 0.1 Å) with the value calculated by using the van der Waals volume that was obtained from the optimized geometry (Supporting Information). The other $r_{\mathbf{1}}$ values (Table 1) were thus calculated by using the same approach.

The heterogeneous ET to **1h** was sufficiently fast to allow us to estimate the rate constant for the follow-up reaction undergone by the electrogenerated radical anion **2h**. The background-subtracted experimental curves were simulated by using the $E_1{}^{\circ}$ and k°_{het} values obtained from the convolution analysis. Since the reduction of **1h** is under mixed kinetic control, which indicates that the kinetics of the follow-up reaction is not too fast, by using the curves obtained at the slowest scan rates, it was possible to estimate a rate constant of 3×10^5 s^{-1}. No such estimate could be possible with the other disulfides.

Oxidation of Thiophenoxides 4. During the voltammetric reduction of disulfides **1**, thiophenoxides **4** form (steps 5 and 6). These anions can be oxidized to the arylthiyl radicals **3** on the positive-going backward scan. Although some accurate electrochemical studies led to the determination or at least estimation of the E°_3 of some **3**/**4** couples in acetonitrile,[24,25] we needed the corresponding values for the solvent of choice, DMF. The anions **4** were generated in situ by voltammetric reduction of the corresponding disulfides. Afterward, on the CV positive-going scan, the irreversible oxidation peak of **4** (reverse of eq 6) could be studied as a function of v. The E°_3 values were eventually obtained by studying the scan rate dependence of the peak[26] and by digital simulation. As expected, the reaction undergone by the radicals is dimerization; in fact, the dependence of the oxidation peak on v and the substrate concentration are 20 and −20 mV per decade, respectively, which are the expected values for the second-order reaction.[26] The results were also in agreement with the observation that the self-reaction of electron rich arylthiyl radicals is relatively slow.[24,27] In particular,

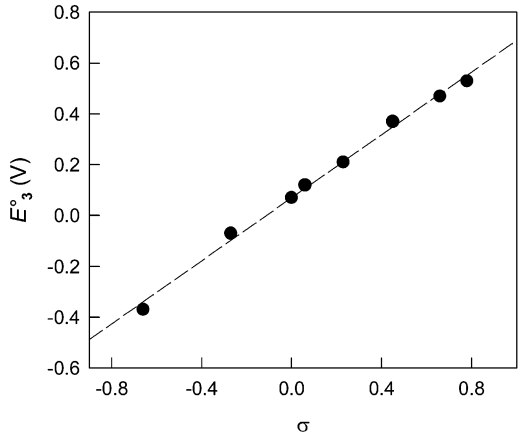

Figure 2. Plot of the E°_3 values against the Hammett substituent coefficient σ. The data were obtained from measurements carried out in DMF/0.1 M TBAP at 25 °C, using a platinum electrode.

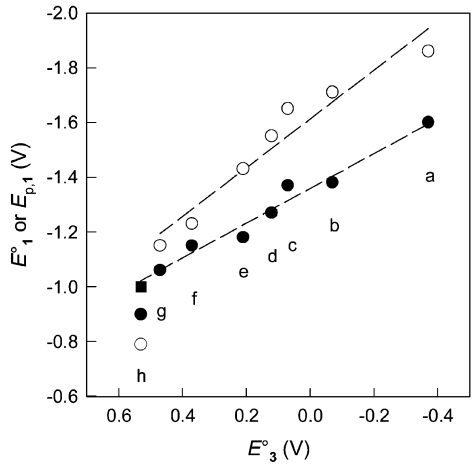

Figure 3. Correlation between the disulfide $E_{p,\mathbf{1}}$ (○) or E°_1 (●) values and the E°_3 values. For the significance of the second E°_1 value of **1h** (■), see text.

some reversibility was evident with the NH_2 derivative even at a scan rate as low as 100 V s^{-1}. The oxidation E_p values and the corresponding E°_3 data are reported in Table 1. A very good Hammett correlation, $E^{\circ}_3 = 0.069 + 0.619\ \sigma$ ($r^2 = 0.995$), is obtained (Figure 2). This result is similar to that previously obtained in one of our laboratories from photomodulated voltammetry experiments carried out in acetonitrile, which is a solvent that has anion-solvation properties similar to those of DMF:[25] $E^{\circ}_3 = 0.103 + 0.548\ \sigma$ ($r^2 = 0.950$).

The E°_3 data are compared in Figure 3 with those obtained for the direct reduction of compounds **1**. The correlation, which was expected because of the similar substituent effects affecting the two series of redox couples, is fairly linear for both the peak potentials ($r^2 = 0.938$) and the E°_1 estimates ($r^2 = 0.966$) (the data of the nitro derivative were not included in the analysis; see below) and thus substantiates the reliability of the E° estimates. The two slopes, 0.89 and 0.63, respectively, are rather different. Once again, this is an indication that when the substituent is made more electron-withdrawing the heterogeneous ET becomes faster and thus the E_p value gets closer to the corresponding E°. With **1h**, this effect is so marked that inversion between the two values is observed. In fact, as previously discussed, the reduction of **1h** takes place under mixed kinetic control. As a final comment, the fact that for **1h**

(23) Kojima, H.; Bard, A. J. *J. Am. Chem.* Soc. **1975**, *97*, 6317.
(24) Andrieux, C. P.; Hapiot, P.; Pinson, J.; Savéant, J.-M. *J. Am. Chem. Soc.* **1993**, *115*, 7783.
(25) Larsen, A. G.; Holm A. H.; Roberson, M.; Daasbjerg, K. *J. Am. Chem. Soc.* **2001**, *123*, 1723.
(26) Olmstead, M. L.; Hamilton, R. G.; Nicholson, R. S. *Anal. Chem.* **1969**, *41*, 260.
(27) (a) Nakamura, M.; Ito, O.; Matsuda, M. *J. Am. Chem. Soc.* **1980**, *102*, 698. (b) Ito, O.; Matsuda, M. *J. Am. Chem. Soc.* **1983**, *105*, 1937. (c) Jeschke, G.; Wakasa, M.; Sakaguchi, Y.; Hayashi, H. *J. Phys. Chem.* **1994**, *98*, 4069.

Scheme 2

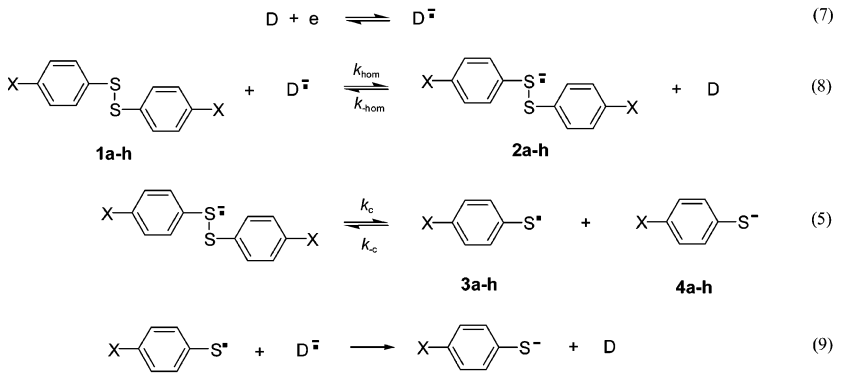

the E_1° value falls far away from the correlation (full circle) points to quite different features of **2h** with respect to those of the other radical anions. The significance of the data point represented as a full square will be discussed later.

Homogeneous ET to Difulfides 1. The mechanism of the homogeneous reduction of disulfides **1** by a generic electron donor is summarized in Scheme 2.

Typical electron donors are radical anions ($D^{\bullet-}$) of aromatic compounds, electrogenerated from their precursors, D (eq 7). D is selected so that its standard potential (E_D°) is more positive than the peak potential of the disulfide. The ET to **1**, eq 8, takes place with the rate constant k_{hom}, while k_{-hom} is the backward rate constant. As discussed above, the so-formed disulfide radical anion **2** cleaves to yield the radical **3** and the anion **4** in a reversible reaction (eq 5). The forward and backward cleavage rate constants are indicated as k_c and k_{-c}, respectively. The final step shown in eq 9 is the reduction of **3** by $D^{\bullet-}$, which is a fast and irreversible reaction associated with a large driving force since the E° of the **3/4** couple is much more positive than the E_p of the precursor disulfide (Table 1). Therefore, the overall stoichiometry is a two-electron indirect reduction of **1** to yield 2 equiv of the corresponding anions **4**.

On the basis of Scheme 2 and by assuming that the reverse of eq 5 can be neglected (see below), we can derive the rate expression describing the disappearance of $D^{\bullet-}$ by applying the steady-state hypothesis to the reactive intermediates **2** and **3** (eq 10).

$$-d[D^{\bullet-}]/dt = \frac{2k_c k_{hom}[\mathbf{1}]}{k_c + k_{-hom}[D]}[D^{\bullet-}] \qquad (10)$$

The competition between the cleavage reaction of eq 5 and the reverse of the ET reaction of eq 8, which is expressed in the denominator of the rate equation, depends on the concentration of D. However, for $k_c \gg k_{-hom}[D]$, the rate-determining step becomes the forward ET process. This situation was encountered with disulfides bearing electron-donating substituents, **1a** and **1b**. On the other hand, if $k_c \approx k_{-hom}[D]$, the disappearance rate of $D^{\bullet-}$ is inhibited by an increase of [D]. Eventually, the cleavage reaction becomes the rate-determining step with the ET step acting as a preequilibrium reaction. Whereas the latter behavior was observed with **1h**, the remaining compounds exhibit a mixed-kinetic behavior.

According to the above kinetic scheme, k_{hom} can be expressed as shown in eq 11, in which

$$\frac{1}{k_{hom}} = \frac{1}{k_d} + \frac{1}{k_{hom}^\circ \exp[(\alpha_{hom}F/RT)(E_1^\circ - E_D^\circ)]} + \left(\frac{1}{k_d} + \frac{1}{Z_{hom}}\right)\frac{1}{\exp[(F/RT)(E_1^\circ - E_D^\circ)]} \qquad (11)$$

k_d is the diffusion-controlled rate constant ($= 10^{10}$ M^{-1} s^{-1}), Z_{hom} is the collision frequency ($= 3 \times 10^{11}$ M^{-1} s^{-1}), k_{hom}° is the homogeneous standard rate constant (the value of the ET rate constant by a generic donor having the same E° as that of the disulfide, i.e., for $\Delta G^\circ = 0$), and α_{hom} is the homogeneous transfer coefficient.[28] Dependent on the magnitude of the three terms, eq 11 and thus the corresponding log k_{hom} versus E_D° graph can be broken down into three main regions, that is, the diffusion, the activation, and the counterdiffusion-controlled zones. Since with the disulfides **1** we could not detect any curvature beyond experimental uncertainty, we employed a simple linear approach to describe the activation-controlled process (the second term of the right-hand side of eq 11). Two typical log $k_{hom} - E_D^\circ$ plots are shown in Figure 4, while the whole series of k_{hom} values are collected in Table 2.

The plots of **1a** and **1b** display an extended activation-controlled region but no indication of a counterdiffusion region at low driving forces, as shown for **1a** in Figure 4a. This outcome can be attributed to a small value of k_{hom}°. On the other hand, the presence of a particularly fast cleavage reaction, taking place within the solvent cage ($k_c > 10^{10}$ s^{-1}), is also liable to extend the activation-controlled region at the expense of the onset of the counterdiffusion-controlled zone. That the latter effect could be relevant for **1a** and **1b** is plausible because of the following two reasons. First, according to the heterogeneous measurements, the intrinsic barriers and the α values of **1a**−**c** should be similar and so should be the corresponding homogeneous free-energy plots. A counterdiffusion zone was observed for **1c**.[8] Second, whereas the kinetics of ET to **1c** depends on the concentration of the mediator (in the range 5−100 mM), which allowed us to estimate $k_c = 5 \times 10^8$ s^{-1},[8] for **1a** and **1b**, even the use of [D] as high as 100 mM did not alter the reaction kinetics, pointing to larger $k_c/k_{-hom}[D]$ ratios. Although the counterdiffusion-controlled zone is absent in the case of **1a** and **1b**, the comparison with the results of **1c** would indicate that k_{-hom} cannot be far away from the diffusion-controlled limit of 10^{10} M^{-1} s^{-1}, at least for donors having the largest values of $-E_D^\circ$. Consequently, the k_c values of the radical anions **2a** and **2b** should be $>10^9$ s^{-1}. This would be in

(28) Andrieux, C. P.; Savéant, J.-M. *J. Electroanal. Chem.* **1986**, *205*, 43.

Table 2. Rate Constants for the Reaction between Radical-Anion Donors and Disulfides **1** in DMF/0.1M TBAT at 20 °C

		log k_{hom} (M^{-1} s^{-1})						
donor	E°_D (V)	**1a**	**1b**[a]	**1c**[b]	**1d**	**1f**	**1g**[a]	**1h**
2,5-diphenyl-1,4-benzoquinone	−0.367							−0.74[c]
1,4-benzoquinone	−0.396							−0.39[c]
2-methyl-1,4-benzoquinone	−0.494							1.45[d]
1,4-naphthoquinone	−0.567						0.11[c]	2.30[d]
2-methyl-1,4-naphthoquinone	−0.649						1.40[d]	
1,2-benzanthraquinone	−0.672		−2.57[c]	−2.62[c]	−1.14[c]	0.30[c,d]	1.96[d]	
2,3-dimethyl-1,4-naphthoquinone	−0.740		−1.59[c]	−0.96[c]	−0.55[c]	1.32[d]	2.60[d,e]	
9,10-dicyanoanthracene	−0.773			−1.47[c]		1.90[d,e]	3.61[d,e]	
9,10-anthraquinone	−0.800	−2.30[c]	−1.32[c]	−0.70[c]	0.32[d]	2.26[d,e]	3.98[e]	
(*E*)-1,2-dibenzoylethylene	−0.830			−0.40[c]	0.60[d]	2.56[d,e]		
2,3-dimethyl-9,10-anthraquinone	−0.870					2.85[d,e]		
1-methoxy-9,10-anthraquinone	−0.880	−1.46[c]	−0.96[c]	0.04[c]	0.98[d]	2.88[d,e]	4.26[e]	
2-chlorophenazine	−0.957	−1.29[c]		0.90[d]			5.18[e]	
4-methoxycarbonylazobenzene	−1.015	−0.43[c]	0.52[d]	1.15[d]	2.09[d]	4.18[e]		
phenazine	−1.090	0.18[c,d]	1.46[d]	2.18[d]	3.10[d,e]	5.34[e]		
3-chloroazobenzene	−1.135		1.76[d]	2.59[d]	3.34[d,e]			
4-chloroazobenzene	−1.183	0.79[d]	2.11[d,e]	2.97[d]	3.72[d,e]			
azobenzene	−1.279	1.51[d]	2.91[d,e]	3.53[d]	4.46[d,e]			
1,4-diacetylbenzene	−1.406				5.83[e]			
2,4′-dimethoxyazobenzene	−1.416	2.61[d,e]	3.89[e]	4.46[d]				
4-dimethylaminoazobenzene	−1.464	3.18[d,e]	4.60[e]	4.96[d]				
tetracene	−1.505	3.88[d,e]						
perylene	−1.613	5.26[e]						

[a] From ref 9. [b] From ref 8. [c] Measured by a potentiostatic method in the presence of 3 mM methyl *p*-toluenesulfonate. [d] Measured by CV. [e] Measured by LSV.

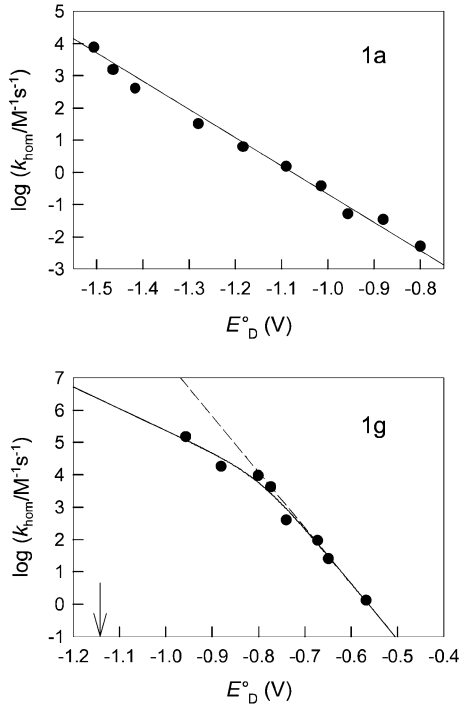

Figure 4. Plot of the logarithm of the homogeneous electron-transfer rate constant against E°_D for the reduction of **1a** (top) and **1g** (bottom) by aromatic radical anions in DMF/0.1 M TBAT at 20 °C.

keeping with the expectation that the amino and methoxy substituents should exert a destabilizing effect on **2a** and **2b**. On these grounds, the minimum standard potential values of **1a** and **1b** can be estimated from the experimental data by simply drawing a line of slope $-1/58$ mV^{-1} ($= -F/(RT \ln 10)$, that is, the slope expected for the counterdiffusion region) from the lowest k_{hom} value (most endergonic reaction) to the diffusion-controlled limit. In this way, the standard potential is calculated by using the last term of eq 11. If we now assume that the absence of the counterdiffusion zone is entirely due to a fast cleavage reaction rather than to a small k°_{hom} value, the uncertainty of the estimated E°_1's is ∼0.12 V.[28] For both **1a** and **1b**, the k°_{hom} values corresponding to either the homogeneously or heterogeneously estimated E°_1's were calculated by linear regression analysis of the rate data.

The plot of **1d** and especially those of **1f** and **1g** display both the activation and the counterdiffusion-controlled regions. This can be interpreted as if the homogeneous intrinsic barriers ($\Delta G^{\ddagger}_{0,hom}$) of these disulfides are somewhat smaller and eventually that the cleavage reaction is slower compared to **1a** and **1b**. Indeed, it was possible using the redox catalysis procedure described previously[29] for the reaction between 1,4-naphthoquinone and **1g** to obtain a rough estimate of the cleavage rate constant of **2g** equal to 2×10^8 s^{-1}. The E°_1, k°_{hom}, and α_{hom} were determined by fitting the experimental points to eq 11. In Figure 4b, which pertains to **1g**, the solid line shows the best fit, the dashed line is the extrapolation of the counterdiffusion component to the diffusion-controlled limit, and the arrow indicates the position of the standard potential. On the basis of the fitting parameters, we could calculate also the k°_{hom} value corresponding to the E°_1 estimated by convolution analysis. Finally, the plot pertaining to **1h** shows only a counterdiffusion region, which immediately gives access to a determination of the standard potential. The lack of an activation zone implies that the $\Delta G^{\ddagger}_{0,hom}$ must be pretty small. A rough estimation of the minimum value of k°_{hom} was tentatively calculated by assuming that the activation component, having a slope of $-1/116$ mV^{-1} (second term of eq 11, $\alpha_{hom} = 0.5$), starts at the point corresponding to the most exergonic reaction. Because of the results obtained by direct electrochemistry, however, we believe that the minimum k°_{hom} value that was estimated by using the above procedure is severely underestimated.

Table 3 shows the homogeneous parameters for the dissociative ET to compounds **1**. From the plots, approximate values

(29) Enemærke, R. J.; Christensen, T. B.; Jensen, H.; Daasbjerg, K. *J. Chem. Soc., Perkin Trans. 2* **2001**, 1620.

Table 3. Standard Potentials and Kinetic Parameter for the Homogeneous Reduction of Disulfides **1** in DMF/0.1 M TBAT at 20 °C

disulfide	$E_1^{\circ\,a}$ (V)	$\alpha_{hom}{}^a$	log $k_{hom}^{\circ\,a}$ (M^{-1} s^{-1})	log $k_{hom}^{\circ\,b}$ (M^{-1} s^{-1})	$\Delta G^{\ddagger\,a,c}_{0,hom}$ (kcal mol^{-1})	$\Delta G^{\ddagger\,b,c}_{0,hom}$ (kcal mol^{-1})	$\Delta G^{\ddagger\,a,d}_{0,i,hom}$ (kcal mol^{-1})	$\Delta G^{\ddagger\,b,d}_{0,i,hom}$ (kcal mol^{-1})
1a	−1.52	0.51	<3.9	4.60	>10.3	9.4	>7.1	6.2
1b	−1.40	0.51	<4.0	3.79	>10.2	10.5	>7.1	7.4
1c	−1.40	0.48	4.52	4.28	9.5	9.8	6.3	6.6
1d	−1.31	0.53	4.86	4.53	9.0	9.5	5.8	6.3
1f	−1.22	0.58	6.49	5.74	6.8	7.8	3.8	4.8
1g	−1.14	0.39	6.34	5.77	7.0	7.8	3.8	4.6
1h	−0.99		>5.9	>5.2	<7.6	<8.6	<4.5	<5.5

[a] From best fit to the homogeneous kinetic data (see text). [b] From best fit to the homogeneous kinetic data, using the convolution E_1° values. [c] Calculated from $k_{hom}^{\circ} = Z_{hom}\exp(-\Delta G^{\ddagger}_{0,hom}/RT)$. [d] Calculated by taking into account the solvent reorganization energy, obtained from the empirical equation $\Delta G^{\ddagger}_{0,s,hom} = 24\,[(2r_D)^{-1} + (2r_1)^{-1} - (r_D + r_1)^{-1}]$. The error associated with these free energy estimates is of the order of 1 kcal mol^{-1}.

Table 4. Energies, Bond Distances, and Morse Parameters of Disulfides **1** and Corresponding Radical Anions **2**

1 or **2**	$BDE_1{}^{a,b}$ (kcal mol^{-1})	$\beta_1{}^{a,c}$ ($Å^{-1}$)	$d_1(S–S)^{a,d}$ (Å)	$BDE_2{}^{a,b}$ (kcal mol^{-1})	$\beta_2{}^{a,c}$ ($Å^{-1}$)	$d_2(S–S)^{a,d}$ (Å)	$\Delta BDE_2{}^{b,e,f}$ (kcal mol^{-1})	$\Delta E_0{}^{a,g}$ (kcal mol^{-1})	$\Delta E_0{}^{f-h}$ (kcal mol^{-1})
a	42.9	2.065	2.095	12.7	2.042	2.893	−2.0	−1.8	−41.4 (6.3)
c	46.2	2.027	2.089	17.7	1.408	2.891	0	−8.3	−47.8 (0)
d	45.9	2.026	2.090	16.2	1.404	2.882	5.3	−15.5	−52.8 (−5.1)
g	43.7	2.246	2.048	22.0	1.336	2.873	5.8	−32.3	−62.9 (−15.1)
h	47.0	2.166	2.047	(47.0)[i]	(1.887)[j]	2.102		−25.1	−67.2 (−19.4)
h[k]				31.2	0.994	2.869	11.2	−37.0	−63.9 (−16.2)

[a] Calculations refer to the gas phase. [b] From the MP2/6-311G*//HF/6-311G* and MP2/6-311G*//UHF/6-311G* theoretical levels (see Experimental Section). [c] Coefficient of the Morse function (HF/6-311G*//HF/6-311G* energies or UHF equivalent). [d] S−S bond distance at the equilibrium geometry. [e] BDE_2 values relative to the value of **2c** in a dielectric having $\epsilon = 37$. [f] Solvent effect: PCM model (see Experimental Section), $\epsilon = 37$. [g] Energy difference between the ground states of the radical anion and the neutral molecule (at the HF and UHF approaches). [h] In parentheses are the values relative to the unsubstituted compound. [i] BDE assumed to be the same as that of the neutral molecule. [j] Obtained by employing the same BDE value of the neutral molecule. [k] The data refer to the radical anion with the S−S bond stretched (see text).

of α_{hom} also could be determined. In agreement with the fact that the homogeneous redox catalysis data refer to a range of smaller driving forces than those explored by direct electrochemistry (the direct reduction of **1** occurs at more negative potentials), the majority of the α_{hom} values are larger than the corresponding heterogeneous α values. The $\Delta G^{\ddagger}_{0,hom}$ were obtained from the relationship $k_{hom}^{\circ} = Z_{hom}\exp[-\Delta G^{\ddagger}_{0,hom}/RT]$, using $Z_{hom} = 3 \times 10^{11}$ M^{-1} s^{-1}. The inner component to the intrinsic barrier, $\Delta G^{\ddagger}_{0,i,hom}$, was obtained by subtracting from $\Delta G^{\ddagger}_{0,hom}$ the solvent reorganization term, $\Delta G^{\ddagger}_{0,s,hom}$. The latter was calculated from the empirical equation $\Delta G^{\ddagger}_{0,s,hom} = 24\,[(2r_D)^{-1} + (2r_1)^{-1} - (r_D + r_1)^{-1}]$,[23,30] in which $r_D = 3.8$ Å is the average radius of the donors.

Theoretical Calculations. Calculations were carried out at different theoretical levels (Experimental Section) on a representative series of disulfides **1a**, **1c**, **1d**, **1g**, and **1h**, their radical anions **2**, and corresponding fragments **3** and **4**. The BDE values and other relevant data of **1** and **2** are provided in Table 4; the calculated total molecular energies of species **1**−**4** and additional results are provided in the Supporting Information. The most significant geometrical parameters calculated for **1** and **2** show that whereas the calculated equilibrium distances of the S−S bond, d(S−S), in the neutral disulfides are in the range 2.047−2.095 Å, those of the radical anions are longer by ∼0.8 Å, being in the range 2.869−2.893 Å. For **1h**, a second stable radical anion structure, having d(S−S) = 2.102 Å, could be also characterized. The energies of the first four LUMOs are reported in Table 5.

Table 4 shows that the S−S BDE values of compounds **1** (BDE_1) are little affected by the para-substituent and that no trend associated with the type of substituent transpires. Conversely, the BDE values of the radical anions **2** (BDE_2), which are markedly smaller than those of the neutral molecules, increase when the substituent becomes more electron-withdrawing. The effect of a dielectric having $\epsilon = 37$ (as the dielectric constant of DMF) on the BDE_1 values is negligible, as expected.[10] It does, however, decrease the BDE_2 values significantly. Whereas the absolute values appear to overestimate the difference between the solvation energy of the radical anion with respect to the smaller anion **4**, the relative BDE_2 trend (Table 4) is similar to that calculated for the gas phase, although the substituent effect is less pronounced.

Table 5. Energies of the Lowest Unoccupied Molecular Orbitals of Disulfides **1**[a]

disulfide	LUMO I (kcal mol^{-1})	LUMO II (kcal mol^{-1})	LUMO III (kcal mol^{-1})	LUMO IV (kcal mol^{-1})
1a	57.6[b]	77.3	84.4	86.7
1c	47.3[b]	75.0	75.7	81.6
1d	44.8[b]	64.5	71.2	74.8
1g	40.4	40.5	54.2	54.5[b]
1h	25.9	26.6	51.3[b]	52.0

[a] Energies at the HF/6-311G*//HF/6-311G* level. [b] Orbital having the most pronounced σ* character.

For the radical anion of the nitro derivative, **2h**, two molecular structures were localized as energy minima. Whereas in the first structure the unpaired electron occupies a molecular orbital that is mainly localized onto one of the two nitro groups and the S−S bond is only slightly stretched (by 0.055 Å), in the second structure the unpaired electron occupies a molecular orbital that is localized onto the S−S bond and the S−S bond is stretched as observed for the other radical anions.

The force constants (k) of the S−S bond (Supporting Information) are markedly smaller in the radical anions than in the corresponding neutral molecules. For **1h**, however, this is true only for the molecular structure having the S−S bond

(30) Donkers, R. L.; Maran, F.; Wayner, D. D. M.; Workentin, M. S. *J. Am. Chem. Soc.* **1999**, *121*, 7239.

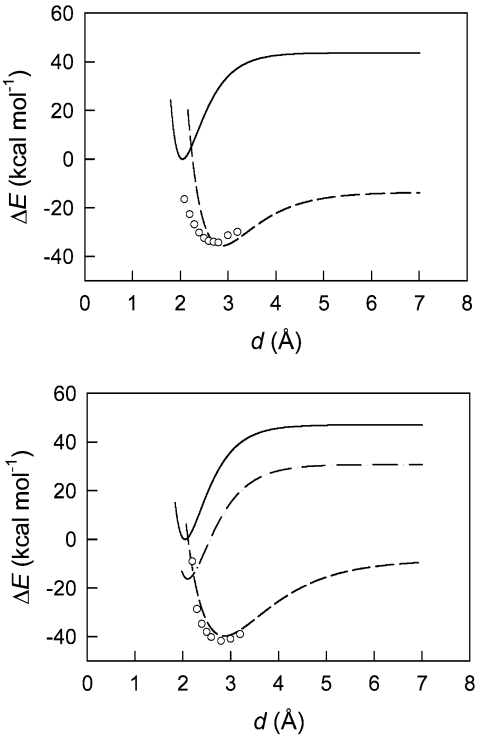

Figure 5. Energy profiles for the S−S bond cleavage in **1g**/**2g** (top graph) and **1h**/**2h** (bottom graph). Morse curves are shown for the neutral molecules (solid lines) and the radical anions (dashed lines; for **2h**, the dash−dot line represents the π^*-radical anion). The data points (○) refer to the corresponding stationary-point calculations.

stretched. The exponential factors of the Morse curve, β, calculated as described in the Experimental Section and reported in Table 4, were employed to describe the energy profiles as a function of d(S−S) in the molecules and radical anions examined. The plots of **1g** and **1h** are reported, as examples, in Figure 5. A number of total molecular energy values were calculated for the radical anions **2c**, **2g**, and **2h** at the UHF/3-21G*//UHF/3-21G* level for frozen S−S distances and by relaxing all the remaining geometrical parameters. Then, the single-point energies were obtained at the MP2/6-311G*//UHF/3-21G* level. This procedure was adopted owing to the high requirements of computer time for relaxing the molecular geometries at the higher theoretical level. For **1c**, to which the procedure applied refers to the MP2/6-311G*//HF/6-311G* level, the calculated points were found to fit very nicely the Morse-like profile. For its radical anion **2c**, the calculated energy values display a trend similar to that of the Morse-like profile, although at S−S bond distances shorter than that of the equilibrium structure of the radical anion the points deviate slightly (the energy is lower) from the corresponding values of the Morse-like profile. A similar although more pronounced trend is observed for the para-cyano derivative **2g**, as shown in Figure 5a, top graph. For the para-nitro derivative **2h**, the calculated energy values fit rather nicely the Morse-like profile of the molecule with the stretched S−S bond (Figure 5b, bottom graph).

Table 4 shows the differences between the energies of the radical anion and the neutral molecule (ΔE_0) along with the corresponding data obtained by simulating the presence of a dielectric having the same dielectric constant of the solvent employed for the experimental measurements ($\epsilon = 37$). The

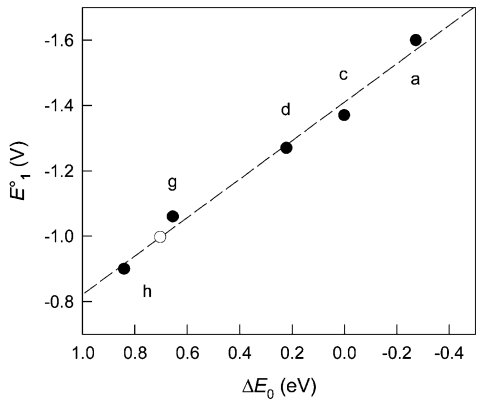

Figure 6. Correlation between the ΔE_0 values and corresponding standard potentials E_1° (●). The energies were corrected for the solvent effect and are relative to compound **1c**. For the second data point of **1h** (○), see text.

two sets of data were calculated at the HF/UHF level of theory.[31] Both in gas and condensed phases, the ΔE_0 value becomes more negative as the Hammett σ increases. Figure 6 illustrates that a good correlation holds between the ΔE_0 (relative solution values) and the electrochemically estimated E_1° values. By using this correlation and the theoretical results for the radical anion of **1h** having longer S−S bond length, for the formation of the latter species, we estimated an "expected" standard potential of −1.00 V. This data point also is shown in Figure 6. Interestingly, once this estimate is plotted as a function of the E° of the **3**/**4** couple, a very good agreement is found with the E_1° versus E_3° correlation already discussed (full square symbol in Figure 3).

Discussion

The kinetic results indicate that the intrinsic barriers for the reduction of the para-substituted diaryl disulfides **1** are as a rule large, although $\Delta G_0^{\ddagger}$ rapidly decreases as the Hammett σ increases. The large $\Delta G_0^{\ddagger}$ values are in full agreement with previous results obtained with a series of dialkyl and alkyl aryl disulfides.[10] The comparison between the heterogeneous and homogeneous results proves to be a very efficient way to substantiate, independently, the reliability of the results and the trends observed. First of all, the satisfactory agreement between the two sets of E_1° values is worth noting (compare Tables 1 and 3). For some compounds, the two sets of potential values are within 40 mV, although larger differences (80−90 mV) can be attributed to the various limitations or experimental uncertainties associated with the homogeneous approach (fast cleavage reactions) or the convolution analysis. Most important, however, our investigation provides the opportunity of gaining important insight into the relationship between the heterogeneous and homogeneous standard rate constants for ET processes characterized by large $\Delta G_{0,i}^{\ddagger}$ values. Previously, there has been few such studies in which the variation in the standard rate constants is significant.[23,32] The k_{het}° and k_{hom}° values estimated for compounds **1a**−**d**,**f**−**g** (by using, for consistency, the same heterogeneously determined E_1°'s) are compared in Figure 7. The figure reveals a remarkably linear correlation (eq 12, $r^2 = 0.971$) and ensures that the observed substituent effect on the

(31) A similar correlation is obtained with the ΔE_0's at the MP2 level, although the effect of the para-substituents seems to be better reproduced at the HF/UHF level of calculation.
(32) Hupp, J. T.; Weaver, M. J. *Inorg. Chem.* **1983**, *22*, 2557.

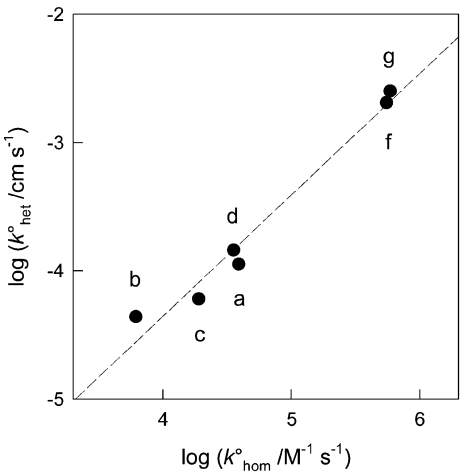

Figure 7. Correlation between the heterogeneous and homogeneous electron-transfer standard rate constants.

intrinsic ET rate is real independently of the fact that the ET is carried out at the electrode or in solution.

$$\log k^\circ_{het} = -8.14 + 0.95 \log k^\circ_{hom} \qquad (12)$$

The data point of **1h**, the k°_{hom} value of which is associated with a large uncertainty, was not included in the correlation. The comparison illustrated in Figure 7 also suggests that the E°_1 values estimated by convolution analysis should not be too far from the real values. Indeed, we have previously discussed that although a quadratic rate/driving force relationship cannot be in principle applied to this type of ET because of differences between the reactant and product Morse curves that may be employed to describe the inner nuclear coordinate (S−S bond elongation), it appears that the E°_1 values estimated for $\alpha \approx 0.5$ should not differ significantly from the actual values.[10] This observation now is supported by the comparison with the homogeneous ET results.

The experimental outcome of Figure 7 can be interpreted by expressing the adiabatic ET rate constants with Eyring-type equations.[33] A relationship between k°_{het} and k°_{hom} is thus derived (eq 13).

$$\log k^\circ_{het} = \log(Z_{het}/Z_{hom}) + (\Delta G^{\ddagger}_{0,hom} - \Delta G^{\ddagger}_{0,het})/(RT \ln 10) + \log k^\circ_{hom} \qquad (13)$$

Since the structural changes occurring in the highly conjugated and rigid D/D$^{\bullet-}$ system (homogeneous ET) are negligible, the contribution of the inner component to the heterogeneous and homogeneous intrinsic barriers is expected to be the same. Thus, eq 13 simplifies to eq 14.

$$\log k^\circ_{het} = \log(Z_{het}/Z_{hom}) + (\Delta G^{\ddagger}_{0,s,hom} - \Delta G^{\ddagger}_{0,s,het})/(RT \ln 10) + \log k^\circ_{hom} \qquad (14)$$

The experimental observation of a linear correlation between $\log k^\circ_{het}$ and $\log k^\circ_{hom}$ having a slope of 0.95 is thus in full harmony with the prediction of eq 14. In addition, the value of the intercept, −8.14, is essentially equal to the theoretical value of $\log(Z_{het}/Z_{hom}) = -7.88$, which is obtained by using the commonly employed average adiabatic prefactors $Z_{het} = 4 \times 10^3$ cm s^{-1} and $Z_{hom} = 3 \times 10^{11}$ M^{-1} s^{-1}. In turn, this would indicate that, for these systems, $\Delta G^{\ddagger}_{0,s,het} \approx \Delta G^{\ddagger}_{0,s,hom}$. On the assumption that the two solvent reorganization energies of the D/D$^{\bullet-}$ couple and the similar-sized **1**/**2** couple are of similar magnitude for the homogeneous reaction, the observed result would further imply that $\Delta G^{\ddagger}_{0,s,het} = \Delta G^{\ddagger}_{0,s,hom,ex}$, where $\Delta G^{\ddagger}_{0,s,hom,ex}$ refers to the homogeneous self-exchange reaction of the **1**/**2** couple. Such a result is thus in much better agreement with the prediction of Hush ($\Delta G^{\ddagger}_{0,s,het} = \Delta G^{\ddagger}_{0,s,hom,ex}$)[34] than to that of Marcus ($\Delta G^{\ddagger}_{0,s,het} = {}^1/_2 \Delta G^{\ddagger}_{0,s,hom,ex}$).[35] It is also worth noting that the calculated $\Delta G^{\ddagger}_{0,s}$ values (to which, because of the various assumptions, we associate an error of about 1 kcal mol^{-1}) lead, for the compounds investigated, to a $(\Delta G^{\ddagger}_{0,s,hom} - \Delta G^{\ddagger}_{0,s,het})/(RT \ln 10)$ term ranging from −0.22 to −0.51, which is indeed a minor correction to the $\log(Z_{het}/Z_{hom})$ term.

To conclude, both the heterogeneous and homogeneous kinetic data point to a common reduction mechanism for disulfides characterized by electron-donating or mildly electron-withdrawing substituents. As σ increases, the inner reorganization energy decreases until, with **1h**, it almost reaches the small $\Delta G^{\ddagger}_{0,i}$ values usually observed with other nitro-derivatives. The heterogeneous and homogeneous results thus concur to indicate that a progressive change of the ET mechanism takes place at positive σ values. The issue now is to understand to which extent the change of the overall reduction mechanism along the series may affect also the cleavage step.

The MO ab initio calculations indicate that the SOMOs of the radical anions **2** are mainly localized onto the S−S bond. For this molecular orbital, however, some stabilizing interaction is possible by losing, partly, its antibonding character thanks to positive phase superposition between the component on the two sulfur atoms. This effect is particularly evident for compounds **2g** and **2h**. For the nitro-derivative **2h**, however, for which we found two energy minima, the SOMO corresponding to the molecular structure having the shortest S−S bond is clearly localized onto one of the substituted phenyl rings. By reasoning within a simplified model in which the electronic structure of these radicals is described in terms of a single electronic configuration, we can derive the following conclusions which can explain, at least on a qualitative level, the behavior of the molecules examined. Reference will be made to the energy of the lowest four unoccupied molecular orbitals (Table 5).

In **1c**, the LUMO I is an orbital having a pronounced S−S antibonding character and lies well down (∼28 kcal mol^{-1}) with respect to the II, III, and IV LUMO orbitals, which have a π^* symmetry. The same occurs in **1a** and **1d**. Thus, since the SOMO also has a pronounced σ^* character, injection of the extra electron does not change substantially the nature of the hosting orbital, although the energy and the S−S bond length change significantly. These results are in full agreement with the experimental results, which point to large inner reorganization energies associated with the ET to these disulfides.

For compound **1g**, the lowest molecular orbitals, I and II, are a nearly degenerate pair of π^* orbitals, while the antibonding

(33) By carrying out a temperature study on compound **1c**, we have previously found that its average Arrhenius prefactor is $\log A_{het} = 3.7$($\log Z_{het} = 3.6$) and thus that its heterogeneous reduction is adiabatic.[10] We now carried out a similar temperature study by using the same disulfide and the radical anion of 3-chloroazobenzene (temperature range −30 to 40 °C) and obtained $\log A_{hom} = 10.3$, which is in reasonable agreement with $\log Z_{hom} = 11.5$.

(34) Hush, N. S. *J. Chem. Phys.* **1958**, *28*, 962. Hush, N. S. *Trans. Faraday Soc.* **1961**, *57*, 557.

(35) Marcus, R. A. *J. Chem. Phys.* **1956**, *24*, 4966. Marcus, R. A. *J. Chem. Phys.* **1965**, *43*, 679.

σ^*(S−S) orbital is IV, which is ca. 14 kcal mol^{-1} higher in energy. Since the incoming electron is accepted by **1g** only when the molecule has undergone significant stretching of the S−S bond, the accepting orbital should reflect a situation in which the original LUMO has progressively changed toward the SOMO equilibrium situation. The latter orbital is one that, once again, has a marked σ^* character. For **1g**, therefore, we have a progressive π^*/σ^* mixing (electronic reorganization) along the reaction coordinate. This mixing is a direct consequence of the S−S bond elongation, which causes the lowering of the σ^* energy, and is in keeping with the fact that a Morse curve description cannot satisfactorily reproduce the situation (energy values at frozen distances) at shorter distances than the equilibrium S−S bond length of **2g**. In other words, at short S−S bond distances, the electronic structure of the radical anion is not properly described by a single determinant wave function; instead, also electronic configurations with the unpaired electron on π^* orbitals should contribute to the electronic structure. Nevertheless, although for this compound the situation is quite different from that of **1a** and **1c**, we still do not have a true $\pi^* \rightarrow \sigma^*$ electron transfer. Experimentally, both heterogeneously and homogeneously, we monitor this new situation, implying extensive electronic coupling at the transition state, through a substantial decrease on the $\Delta G^{\ddagger}_{0,i}$ value with respect to the values of disulfides bearing less electron-withdrawing substituent.

The trend evidenced with **1g** becomes much more pronounced with the nitro derivative, **1h**. Whereas the LUMOs I, II, and IV are symmetrical π^* orbitals, the LUMO III is an essentially pure σ^* orbital. However, the energy difference between the lowest unoccupied orbitals of π^* symmetry and the σ^* orbital is now large enough, 25 kcal mol^{-1}, to justify for the radical anion the separation of a molecular structure having a pronounced π^* character. The presence of two minima characterized by different S−S bond lengths is thus responsible for having a successive intramolecular ET reaction. This is, however, not an intramolecular concerted dissociative ET, as observed, say, with peroxide acceptors and donor moieties bearing a nitro[36] or even a cyano[36a] aryl substituent. In fact, the unpaired electron, which is first accommodated into a π^* antibonding orbital that is entirely localized onto one of the two nitrophenyl groups, is then transferred into the σ^* S−S orbital to form a different radical anion. This new σ^*-type radical anion is similar to those already described for the other disulfides. According to our correlations and corresponding estimates, the σ^* radical anion of **1h** has an E° which is 0.10 V more negative than that of the π^* radical anion. Within this framework, the electrochemically calculated rate constant of 3×10^5 s^{-1} would thus correspond to the $\pi^* \rightarrow \sigma^*$ electron transfer. Finally, an endergonic S−S bond cleavage takes place. A similar mechanism for the cleavage of radical anions of aromatic halides has recently been proposed.[29,37] This second antibonding orbital of **2h** maintains some contributions from the aryl systems. This partial delocalization, which, as already mentioned, is detectable at different degrees also with the other disulfides, is responsible for the calculated increase of the bond energies of the disulfide radical anions as the Hammett σ increases.

The cleavage free energies, which for the endergonic dissociations undergone by radical anions **2** correspond to the bond dissociation free energies ($BDFE_2$), can be extracted from the experimental results by using eq 15.

$$BDFE_2 = FE_1^\circ - FE_3^\circ + BDFE_1 \qquad (15)$$

The expression in eq 15 is obtained from a thermochemical cycle.[5] Thus, the difference between the BDFEs of **1** and **2**, ΔBDFE, is obtained directly as $F(E_3^\circ - E_1^\circ)$ (Table 1). The corresponding ΔBDE value is similarly obtained, the calculated average entropy change associated with the formation of disulfide radical anions at 25 °C being $T\Delta S = 2.5$ kcal mol^{-1}.[10] The ΔBDFE values seem to increase slightly as the Hammett σ increases. It is not clear, however, whether this trend is real, as the theoretical $BDFE_1$ values (which can be obtained from the theoretical BDE_1 data by adding a common $T\Delta S$ correction of 8.5 kcal mol^{-1}) do not display any specific substituent effect. The reliability of the trend is also affected by the experimental uncertainties associated with the E_3° and, particularly, E_1° values. On the other hand, we found previously (at a lower level of theory) that the BDE_1 increases slightly as the electron-withdrawing character of the substituent increases.[5] This is consistent with data pertaining to para-substituted thiophenols.[38] Already it was suggested that electron-withdrawing groups stabilize the S−S bond by decreasing the electric repulsion between the electrons on the sulfur atoms.[39] Therefore, despite the theoretical results obtained for the BDE_1 values in the present investigation, it is conceivable that a similar substituent effect on $BDFE_1$ and $BDFE_2$ may well cause the ΔBDFE values to vary very little within the investigated series. Therefore, since the theoretical results suggest that the $BDFE_2$ value increases as the Hammett σ increases, the $BDFE_1$ also should experience a similar substituent effect. We believe that this trend is quite reasonable, as it is related to a progressive increase of the involvement of the aryl systems in stabilizing the SOMO: the greater the delocalization of the unpaired electron, the larger the S−S bond energy becomes.

As to the thermally activated endergonic cleavage of the radical anions **2**, the solvent reorganization accompanying the process should increase slightly as the para-substituent becomes more electron-withdrawing. In other words, less reorganization is required when the negative charge of the cleaving radical anion is mostly localized onto the elongated S−S bond and thus the SOMO has a pronounced σ^* character: Since the cleavage yields anion **4**, whose charge is localized onto a sulfur nonbonding orbital, the negative charge remains essentially where it was before the cleavage itself. On the other hand, the entropy change associated with the formation of the fragmentation products is constant along the series. Therefore, besides the solvent reorganization, we may relate the S−S bond cleavage rate directly to the difference between the BDE_2 values. From this viewpoint, according to the picture emerging from the theoretical calculations the cleavage rate constant should thus become smaller as the Hammett σ increases. The solvent

(36) (a) Antonello, S.; Maran, F. *J. Am. Chem. Soc.* **1999**, *121*, 9668. (b) Antonello, S.; Crisma, M.; Formaggio, F.; Moretto, A.; Taddei, F.; Toniolo, C.; Maran, F. *J. Am. Chem. Soc.* **2002**, *124*, 11503.
(37) Pierini, A. B.; Duca, J. S., Jr.; Vera, D. M. A. *J. Chem. Soc., Perkin Trans. 2* **1999**, 1003.
(38) (a) Bordwell, F. G.; Zhang, X.-M.; Satish, A. V.; Cheng, J.-P. *J. Am. Chem. Soc.* **1994**, *116*, 6605. (b) Armstrong, D. A.; Sun, Q.; Schuler, R. H. *J. Phys. Chem.* **1996**, *100*, 9892.
(39) Tagaya, H.; Aruga, T.; Ito, O.; Matsuda, M. *J. Am. Chem. Soc.* **1981**, *103*, 5484.

reorganization effect would contribute to slow the cleavage in the same direction. These predictions are in keeping with the conclusion, based on the homogeneous kinetic results, that the cleavage rate constant k_c tends to decrease as σ increases: We found that k_c is $> 10^9$ (**2a,b**), 5×10^8 (**2c**), and 2×10^8 s^{-1} (**2g**). Since another reaction seems to affect the lifetime of **2h** (the intramolecular $\pi^* \rightarrow \sigma^*$ ET), we cannot estimate the corresponding k_c value.

Based on the self-consistency of our theoretical calculations and experimental results, including previous related work,[10] we may conclude that reasonable predictions on both the kinetics and thermodynamics of the reduction of disulfides are possible by carrying out specific electrochemical experiments. Generally, for most chemical systems, the groups bridged by S−S bonds are nonactivated functional groups, such as in proteins. With these disulfides and with aryl disulfides bearing electron-donating or mildly electron-withdrawing groups, the large inner reorganization experienced by the molecule upon ET leads to the formation of loose radical anion species in which the SOMO is heavily localized onto the frangible bond. Consequently, the S−S bond energy is rather small, and the cleavage rate constant, large. When the extent of delocalization of the unpaired electron onto the aryl system increases, the reorganization associated with the formation of the radical anion decreases and the S−S bond cleavage rate decreases slightly. The nitro-substituted disulfide **1h** provides the opposite limit. Whereas the electrochemical reduction involves the nitro group in a very usual fashion and thus very limited inner reorganization is required, a nondissociative type intramolecular ET then ensues, leading to the actual radical anion undergoing the cleavage. The intramolecular ET entails significant S−S bond elongation to form a species whose antibonding orbital is quite similar to the SOMO of the other diaryl disulfides, particularly those bearing electron-withdrawing groups. The latter compounds, as described for **1g** and valid also for **1f**, provide a transition behavior in that the S−S bond elongation along the reaction coordinate alters the relative energies of the unoccupied orbitals to a point at which significantly different features characterize the LUMO and the SOMO, resulting in extensive coupling at the transition state and moderate intrinsic barriers. The overall picture just described relates to disulfides that are not involved in rigid or semirigid networks, such as in peptide systems and proteins. Further work is now required to understand whether specific environmental features may affect the formation and cleavage of S−S bonds.

Acknowledgment. This work was financially supported by the University of Padova (research project A.0EE00.97), the Ministero dell'Istruzione, dell'Università e della Ricerca (MIUR), and the Statens Naturvidenskabelige Forskningsråd. We are also grateful to the Centro di Calcolo Interuniversitario dell'Italia nord-orientale (CINECA) for computing facilities. Dedicated to Professor Sergio Roffia on the occasion of his retirement.

Supporting Information Available: Molecular geometries (Cartesian coordinates) of the relaxed geometries, relevant energies and additional geometrical features, and single-point frozen core MP2 energies. This material is available free of charge via the Internet at http://pubs.acs.org.

JA036380G